American Journal of Materials Science 2021, 11(2): 48-55
DOI: 10.5923/j.materials.20211102.02

Reduction Effect of Exposure to Ultraviolet Radiation Graphene Oxide Aqueous Suspensions with Different pH Values

Plínio Fernandes Borges Silva[1,*], Lúcia Emília Letro Ribeiro[2], Vinícius Meirelles Mendonça[1], Sidney Nicodemos da Silva[1]

[1]Department of Materials Engineering, Federal Institution of Technological Education of Minas Gerais, Belo Horizonte, Brazil
[2]Department of Chemistry, Federal Institution of Technological Education of Minas Gerais, Belo Horizonte, Brazil

Abstract In this work, it was analyzed the photocatalyst reduction of graphene oxide radiated by ultraviolet (UV) light with three different pH values and without any photoactivatable nanoparticles or photo-initiator chemicals. A pristine graphene oxide was dispersed in an aqueous solution and exposed to UV light for five hours with constant stirring and controlled temperature. After the exposure process, the solutions were put in an oven at 120℃ for 8 hours for the solvent evaporation. To investigate possible changes in the graphene oxide morphology a Scanning Electron Microscopy (SEM) was applied. Also, during the SEM analysis X-ray spectroscopy by energy dispersion (EDS) was performed to obtain a semi-quantitative chemical characterization. To complement the chemical characterization, the Fourier transform infrared (FTIR) spectroscopy, Raman spectroscopy technique and thermogravimetric analysis (TGA) were performed. Lastly the change in the microstructure was determined by X-ray diffraction (XRD). The characterization showed a decrease in the oxidation degree of the graphene oxide submitted to the process proposed. Thus, the results indicated that the acid environment improved the reduction of the oxygen-functional groups present in the graphene oxide. This work collaborates to the possibility of the use of UV-light exposure to obtain reduced graphene oxide with different degrees of oxidation.

Keywords Graphene Oxide, Reduced Graphene Oxide, Photocatalyst Reduction, UV light Exposure

1. Introduction

Graphene oxide (GO) is a carbon-based nanomaterial that has in its structure the presence of oxygen atoms and other oxygenated chemical groups, granting it different properties from graphene. This structure derived from graphene is characterized by the presence of chemical functional groups such as: hydroxyl, carbonyl and epoxy, on the surface and/or at the ends of the carbon sheet [1], [2]. These oxygen-functional groups (OFGs) are remnants of the GO production process, called chemical exfoliation. In general, GO is obtained through an intense oxidation of graphite in an extremely acidic solution in the presence of different oxidizing chemical agents, a method initially developed by Hummers, Offeman 1958 [3], [4].

In addition, the chemical exfoliation process, due to its low cost and high efficiency, is used to obtain a version of graphene oxide with properties closer to graphene [5], [6]. Nevertheless, graphene oxides (GOs) have advantages over graphene in terms of better solubility and stability in aqueous media [7], [8]. The reduced graphene oxide (rGO) is obtained after a process of reduction of the graphene oxide for the removal of OFGs and restoration of the hexagonal sp2 structure of graphene [9]. The best-known types of GO reduction are thermal [10], [11], chemical [12], [13], electrochemical [14], [15] and photocatalytic reduction [16]. Each process has their own characteristics and limitations, therefore, there is no superior method among them [17].

The photocatalytic reduction process consists of the use of electromagnetic radiation to remove the oxygen-functional groups. This process is known for having two different paths for reduction: 1) using photoactivatable inorganic nanoparticles and, 2) using activated photo-initiator compounds [18]. Radiations in microwave, visible, ultraviolet and gamma spectra have already been tested in this process by other authors [19]–[22]. In general, electromagnetic radiation interacts with the agents and the GO in order to generate the right conditions for the removal of the OFGs from the graphene oxide structure.

The photoactivatable inorganic nanoparticles approach is based on the capability of specific particles to generate electron-hole pairs when irradiated by specific

* Corresponding author:
plinio.eng1707@gmail.com (Plínio Fernandes Borges Silva)
Received: Sep. 21, 2021; Accepted: Oct. 14, 2021; Published: Oct. 30, 2021
Published online at http://journal.sapub.org/materials

electromagnetic wavelengths. This excited state is capable of inducing the reduction in the GO and generate rGO/nanoparticles hybrids [23]. Titanium dioxide, silver nanoparticles, and zinc oxide are some well-known examples of nanoparticles tested for this purpose [24]–[26].

Whereas, the use of photo-initiator chemical compounds for the reduction of graphene oxide is based on the possibility that by electromagnetic radiation. Many different compounds were tested for this purpose such as ascorbic acid, polyvinyl pyrrolidone, sulphite, and even green alternatives such as tea leaves extract [21], [27]–[29]. These compounds create free-radicals that can interact with the OFGs extracting them from the GO's structure [30].

Research on the investigation of the photocatalytic reduction without the use of any photoactivatable nanoparticles or photo-initiator chemicals have been limited. Guardia et al. 2012 [31] investigated the capability of the reduction of graphene oxide in aqueous solution irradiated by UV light. The results showed that the UV light radiation achieved lower oxidation states on the GO dissolved only in deionized water.

The aim of this work is to contribute to the study of the photocatalytic reduction of graphene oxide radiated by ultraviolet (UV) light without any photoactivatable nanoparticles or photo-initiator chemicals, evaluating aqueous solutions with alkaline, neutral and acidic pH. Thus, this study proposes a simplified process, without controlled atmosphere, and with the possibility to manufacture reduced graphene oxides with a desirable level of oxidation.

2. Experimental

2.1. UV-Radiation Exposure Process

The exposure process was done using 200 mg of graphene oxide (pristine GO) provided by the research center Centro de Tecnologia em Nanomateriais e Grafeno CTNano (Belo Horizonte, Brazil) solubilized in 200 mL of a solution composed of deionized water and isopropyl alcohol (50% v/v), achieving the concentration of 1 g/L. From this initial dispersion, three samples were made with different pH adding HCl 1 mol/L and NaOH 1 mol/L to the acidic and alkaline media, respectively. Table 1 shows the detailed solution composition for each sample.

Then, the samples were subjected to vigorous magnetic assisted stirring for 1 hour and then exposed to UV radiation in a reactor built with 7 Philips 12 W UV-C radiation lamps, λ = 100 to 280 nm (Figure 1-a). During the entire photoreduction process, the solution remained vigorously stirred in a 250 mL jacketed beaker (Figure 1-b), which allows the external circulation of refrigeration liquid (water at 4℃), through a connection to a Water Chiller.

The distance between the beaker and the lamps was approximately 25 centimetres. After a 5 hours radiation exposure, the solution was removed from the reactor and taken to an oven at 120℃ for 8 hours for the solvent evaporation.

2.2. Characterization

The morphological structure was obtained by scanning electron microscopy (SEM) analysis with SHIMADZU SSX-550 equipment with a tungsten filament and Acc Voltage of 15,0 kV. During the SEM analysis, X-ray spectroscopy by energy dispersion (EDS) was performed to obtain a semi-quantitative chemical characterization of the material. To detect peak displacement in the samples diffractograms, an X-ray diffraction (XRD) analyzes were performed on a SHIMADZU XRD-7000 device using a copper target (CuKα, and λ = 0.15406 nm) at 40 kV and 30 mA. The analysis was conducted with angle range of 2θ = 5° – 50° and scan speed of 2 o/minute.

The presence of oxygen-functional groups was analyzed by Fourier transform infrared (FTIR) spectroscopy technique performed on the Perkin Elmer FTIR Frontier device, with a wavelength range of 4000-650 cm^{-1}. The graphene structural organization was measured using the Raman spectroscopy, performed on the WiTec Alpha300 device with the λ = 532 nm wavelength laser.

The weight loss due to the photoreduction of GO was measured by thermogravimetric analysis (TGA), performed on the HITACH STA7000 series equipment, with a sensitivity of 0.2 µg and in an inert atmosphere of N2. The analysis was conducted with a maximum temperature of 1000℃ and 10℃/min of temperature increment on a platinum crucible.

3. Results and Discussion

As shown in the figure 1, the Pristine GO had the aspect of a solid foam with visible porosity. The A-2 and B7 samples turned out into identical flat sheets of solid and brittle material.

Table 1. Samples with pH values and detailed composition of the solutions

Sample	pH	Detailed Composition
A-2	2	100mL Deionized H_2O + 100 mL isopropyl alcohol + ~1mL de HCl 1mol/L
B-7	7	100mL Deionized H_2O + 100mL isopropyl alcohol
C-12	12	100mL Deionized H_2O + 100mL isopropyl alcohol + ~1mL de NaOH 1mol/L

The sample C-12 with pH = 12 was not capable of solubilize the GO used, therefore it was not submitted to the photoreduction process. This result is a contrast with other works such as [31], [32]. However, the complex nature of the composition of graphene oxide due to its variety of fabrication compounds, can hinder the stability of GO in different solvents with a large range of pH by unexpected functionalization [33]. Thus, unexpected similar results of unstable solubility with alkaline pH can also be found in the literature [34], [35].

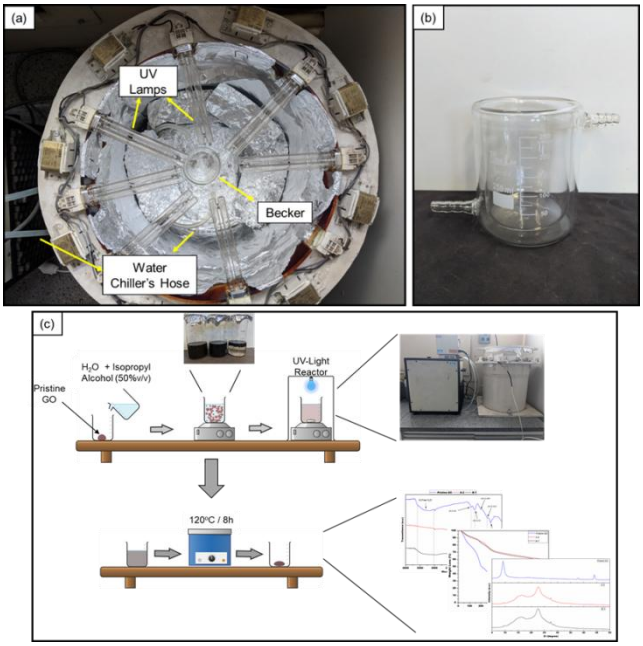

Figure 1. Illustration of the Experimental Setup (view from above): (a) UV Exposure Reactor (b) Jacketed Beaker (c) Graphical Abstract

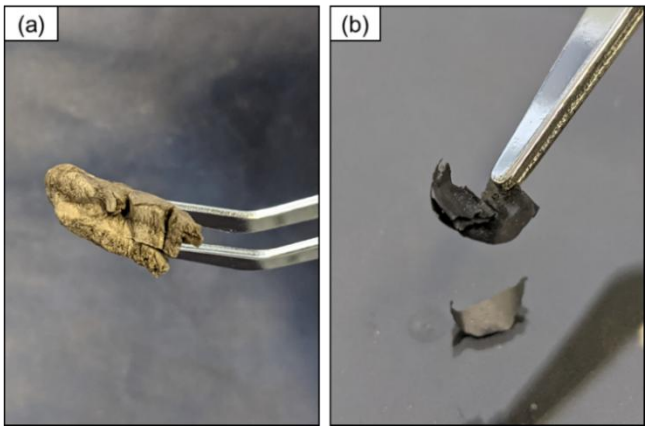

Figure 2. Images of the samples: (a) Pristine GO (b) A-2

3.1. SEM/EDS Analysis

The SEM images (figure 3) present the morphology of the samples before (Pristine GO) and after the photoreduction process. It is possible to notice that the pristine GO had a cohesive and porous structure, with the GO nanosheets connected to each other (figure 3-a). This morphology can be attributed as a result of the lyophilization process to obtain solid GO from a solution, in accordance with the structures reported by Yu et. al. (2015) and Tang et al (2019) [36], [37].

The samples A-2 and B-7 (figure 3-b and 3-c), on the other hand, presented a cohesive and planar structure with the presence of folds of GO nanosheets over the entire surface. In sample B-7 (figure 3-c), a remaining porosity of the pristine GO was identified. This characteristic can be considering as an intermediate result in comparison with sample A-2. Besides that, in the sample A-2, the surface was more cohesive with no porosity. Also, the surface was marked with the presence of bigger folds in GO nanosheets.

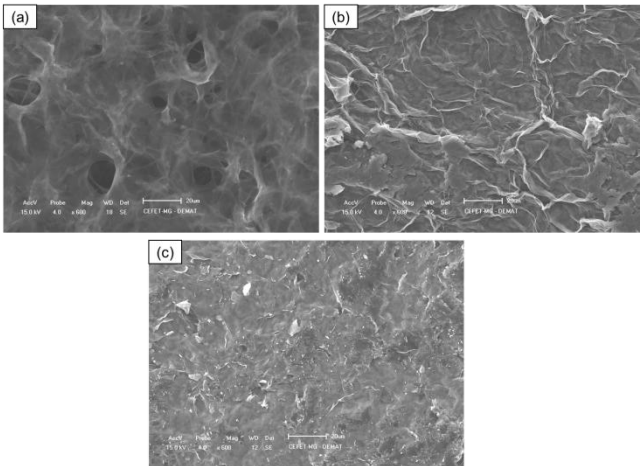

Figure 3. SEM images of the samples: (a) Pristine GO (b) A-2 (c) B-7

The EDS analysis was used to obtain the concentrations of carbon and oxygen present in three regions of each sample. With that, it was possible to calculate the C/O concentration ratio for these regions and measure the local reductive capacity of the process. The average results of the concentrations measured and the C/O ratio for each sample are shown in table 2.

Table 2. EDS analysis of the GO before and after the UV Exposure (%wt)

Sample	Region	C	O	Average of C [SD]	Average of O [SD]	C/O Ratio
Pristine GO	1	42.0	58.0	40.8 [1.1]	59.2 [1.1]	0.6
	2	40.5	59.5			
	3	39.8	60.2			
A-2	1	51.9	48.1	58.8 [5.5]	41.2 [5.5]	1.4
	2	58.6	41.4			
	3	56.2	43.8			
B-7	1	53.7	46.3	55.6 [3.4]	44.4 [3.4]	1.2
	2	64.7	35.3			
	3	57.9	42.1			

The results in Table II showed a considerable increase in the C / O ratio of the regions measured in the samples submitted to the UV exposure process. This outcome can be attributed to the removing of the OFGs present on the surface of the material, giving evidence to the skeletal carbon chain of the GO. Also, it can be observed that the C/O ratio increased with a decrease in the pH of the solution, thus indicating an increase in the efficiency of the photoreduction process in acidic media.

3.2. FTIR Spectroscopy

Figure 4 shows the results of the FTIR analysis of the GO samples and the identification of vibrational bonds peaks. The result of the FTIR analysis of the pristine GO sample (Figure 4) revealed peaks related to the vibration of chemical bonds of the oxygen-functional groups present in the graphene oxide. The peaks can be attributed bonds [10],

[15], [38]–[40]:

(I) ~3250 cm^{-1}: Free H_2O molecules vibration;
(II) ~1730 cm^{-1}: Stretching of carbonyl and/or carboxyl groups (C=O);
(III) ~3250 cm^{-1}: Free H_2O molecules vibration;
(IV) ~1730 cm^{-1}: Stretching of carbonyl and/or carboxyl groups (C=O);
(V) ~1600 cm^{-1}: Skeletal carbon vibration of unoxidized graphitic domain (C=C);
(VI) ~1380 cm^{-1}: Alcoholic groups vibration (C-OH);
(VII) ~1150 cm^{-1}: Vibration of epoxy (C-O-C) and phenolic groups (C-OH);
(VIII) ~1055 cm^{-1}: Alkoxy groups vibration (C-O).

As it can be seen, the curves of the samples after the exposure process showed a significant decrease in the intensity of the peaks highlighted.

In addition, the sample A-2 had a more drastic decrease in the peak's intensities, in comparison with B-7. So, the B-7 sample as presented in the SEM analysis can be considered as an intermediate result between the pristine GO and the A-2 sample. Corroborating to the positive influence of an acid environment on the efficiency of the process as detected locally by EDS spectroscopy.

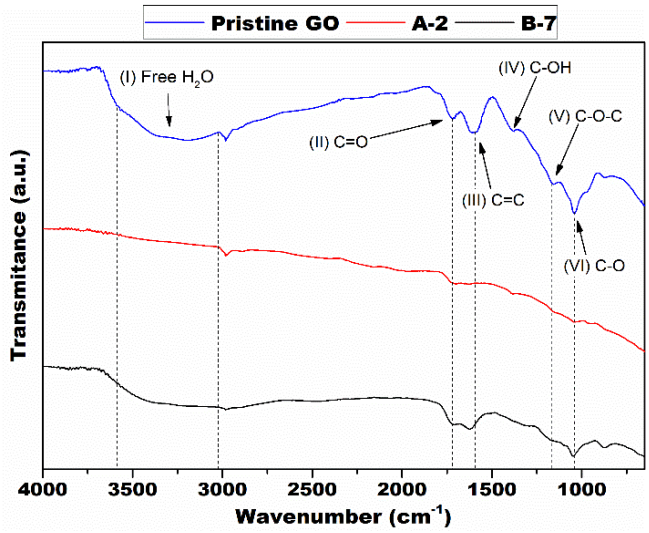

Figure 4. FTIR spectroscopy curves with highlighted peaks

3.3. Raman Spectroscopy

The Raman spectroscopy graphs of the samples where the D, G, 2D and G' bands of carbon nanomaterials could be identified in the figure 5.

The D and G bands are found in the literature in displacements 1350 cm^{-1} and 1580 cm^{-1} respectively, however, as it is shown in figure 5 the peaks appeared with a red shift [41]. This phenomenon is commonly found in graphene oxides because of the OFGs present in its structure. The functional groups can alter the interaction between the laser and the phonons of the D and G bands. One explanation for this phenomenon is the large number of C=C double bonds isolated by oxygenated functional groups [14].

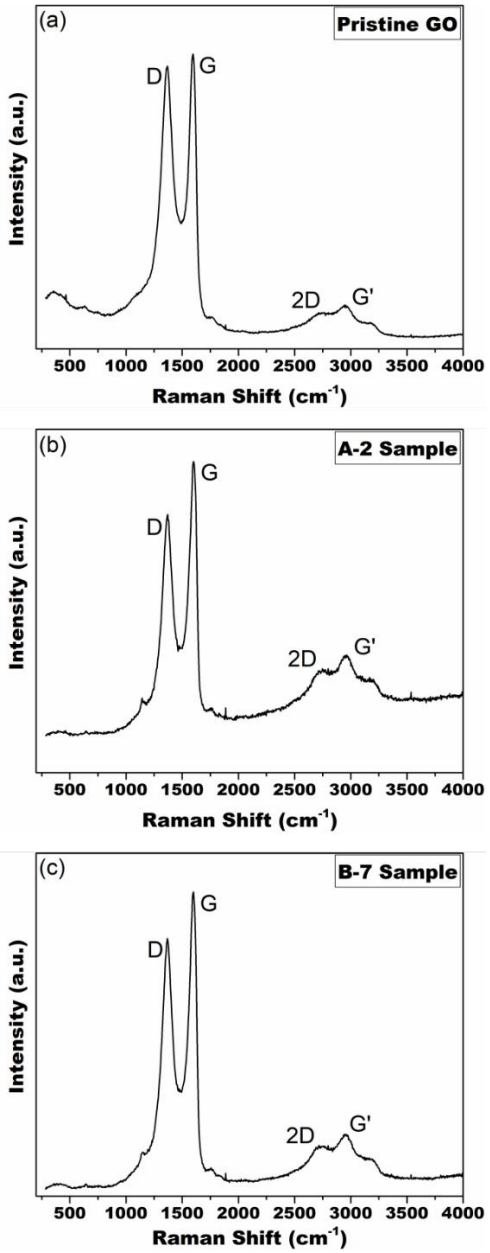

Figure 5. Raman spectroscopy of the samples: (a) Pristine GO (b) A-2 (c) B-7

In addition, it was possible to identify other characteristic peaks of carbon nanomaterials: the band 2D (~ 2700 cm^{-1}) and Band G' (3000-3200 cm^{-1}), which are much more intense in graphene compared to graphite. The peak shift in graphite is a result of interactions between the stacked graphene layers which has a tendency to shift the bands to higher frequency. The G' band in a single layer graphene oxide spectrum fits a single curve, while the curve adjustment observed in this study, demonstrate that after processing, several underlying bands form in the spectrum of a graphite [42].

These bands are the result of different interactions between layers that occur at different depths within the graphene oxide. Therefore, these bands can be related to the number of layers present in carbon nanomaterials [14], [41].

The I_D/I_G ratio of the samples is the parameter commonly used to relate ordered/disordered structures of the carbon nanomaterials.

Through table 3, it is possible to notice that the samples did not show a significant variation in the ID/IG index after the applied process, which is uncommon in graphene oxide reduction processes.

However, this phenomenon can happen in some reduction processes due to the balance of two opposing mechanisms. On one hand, there is an increase in the disorganization of the microstructure, due to the elimination of oxygenated functional groups and the consequent appearance of defects.

On the other hand, the organization of the structure is favoured through the relaxation of the network parameters and the elimination of disordered carbons [10], [15], [43]. Therefore, the applied process was able to both eliminate the oxygenated functional groups from the GO structure, and repair the organization of the skeletal carbon chain.

Table 3. The I_D/I_G ratio of the samples

Samples	I_D/I_G
Pristine GO	0.98
A-2	0.95
B-7	0.96

3.4. X-Ray Diffraction

The diffractograms of the samples (figure 6) show a peak displacement caused by the photoreduction process.

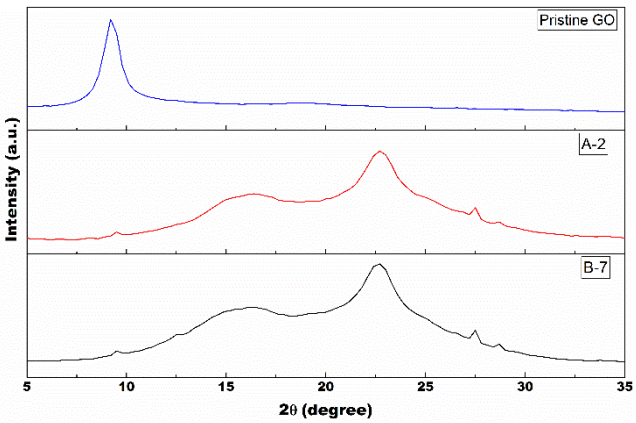

Figure 6. Diffractograms of the samples showing a peak shift after the UV radiation exposure

The Pristine GO shows a classic graphene oxide peak at 2θ = ~9° representing a basal reflection of (001) and d-spacing around 0,96 nm [44]. These characteristics are due to the incorporation of the oxygen-functional groups which increase de spacing between the graphene layers.

After the photoreduction process the graphite peak (2θ = ~26°) appears shifted to the left at 2θ = ~22°, and the graphene oxide peak is also shifted to 2θ = ~16°. The d-spacing for both peaks are 0,40 and 0,55 nm respectively, which indicate a recovering of the graphitic network in the GO by the removal of the OFGs [43], [45], [46]. When a high degree of reduction is reached, these peaks merge in one narrow peak at 2θ = 27° with a d-spacing around 0,3 [10].

Therefore, the proposed process was able to reduce, at least partially, the number of oxygenated functional groups of the material, which was also appointed with the EDS and FTIR analysis.

3.5. Thermogravimetry Analysis

Figure 7 shows the result of the thermogravimetry analysis showing a decrease of weight loss after the applied process. The TGA results show an intense decrease in weight loss of the samples submitted to the photoreduction process in relation to the pristine GO.

The Pristine GO had a weight loss of 76% while the A-2 and B-7 samples had 41% and 42%, respectively. This result can be considered a measurement of the mass released by the reduction of the OFGs from the sample by the purposed process. The curves reveal three very distinct mass loss regions, between temperatures 25 to 120℃, 150 to 200℃ and 200 to 300℃.

These regions can be related to the evaporation of water linked to the samples, the decomposition of less stable oxygenated functional groups (carboxyl, anhydride, etc.) and the decomposition of more stable groups (carbonyl, phenol, etc.), respectively [43], [47], [48]. It is worth mentioning that the decreasing of the intensity (or weight loss) related to the OFGs from the pristine GO to the UV-exposed samples was also detected by the FTIR analysis.

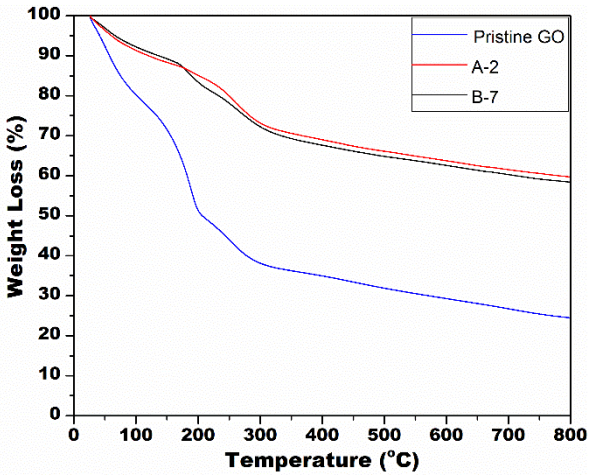

Figure 7. TGA results of the samples before and after the UV radiation exposure

4. Conclusions

In summary, this work studied the photocatalytic reduction of graphene oxide by UV radiation without the use of any photoactivatable nanoparticles or photo-initiator chemicals. Also, it was tested the influence of three different pH on the performance of the proposed process. First, the sample with alkaline pH was not able to solubilize the GO used, making in unviable for the proposed process. Then, the

results confirmed that the graphene oxide solubilized in solutions with acid and neutral pH was partially reduced. The UV light was able to interact with OFGs on the surface of the GO particles in suspension, providing enough energy to extract them from the nanoparticle. The characterization techniques proved a significant variation from the pristine GO to the after-exposure samples. The XRD analysis presented a peak shift from 2θ = ~9° to 2θ = ~16° merging with the graphene peak at 2θ = ~22°, which is well-known result for the reduction of GO. Also, the reduction of weight loss from 76% for Pristine GO to ~40% for the irradiated samples measured by TGA confirmed the reduction capability of the process. The pH influence in the photocatalytic reduction was confirmed by FTIR and EDS analysis. The measurement of carbon and oxygen concentration of regions of the samples by EDS spectroscopy determined a local C/O ratio that confirmed an increase of the oxygen reduction for the sample with acid pH. In addition, the FTIR spectroscopy showed a reduction in the peaks related to the bond of the OFG's for the irradiated samples, and this reduction was more drastic for the acidic pH sample. Thus, the analysis of the Raman spectroscopy of the samples suggests that the purposed process was able to maintain the defect level of the GO used, by a balance of energy for both extraction of the OFGs and restauration of the graphene carbon matrix. Finally, the proposed process presents itself as an easier and straightforward way of reducing GO. Furthermore, it allows the possibility of manufacture rGO with different levels of oxidation, that can be designed to be a perfect fit in different applications.

ACKNOWLEDGEMENTS

This study was financed in part by the Coordenação de Aperfeiçoamento de Pessoal de Nível Superior – Brasil (CAPES) – Finance Code 001. This work was also supported by the Centro de Educação Tecnológica de Minas Gerais (CEFET-MG), Centro de Tecnologia em Nanomateriais e Grafeno (CTNano), Conselho Nacional de Desenvolvimento Científico e Tecnológico (CNPq) and Fundação de Amparo à Pesquisa do Estado de Minas Gerais (FAPEMIG).

REFERENCES

[1] Z. Liu, T. Rios-Carvajal, M. Ceccato, and T. Hassenkam, "Nanoscale chemical mapping of oxygen functional groups on graphene oxide using atomic force microscopy-coupled infrared spectroscopy," *J. Colloid Interface Sci.*, vol. 556, pp. 458–465 (2019).

[2] T. Szabó *et al.*, "Evolution of surface functional groups in a series of progressively oxidized graphite oxides," *Chem. Mater.*, vol. 18, no. 11, pp. 2740–2749 (2006).

[3] W. S. Hummers and R. E. Offeman, "Preparation of Graphitic Oxide," *J. Am. Chem. Soc.*, vol. 80, no. 6, pp. 1339–1339, Mar. (1958).

[4] P. P. Brisebois and M. Siaj, "Harvesting graphene oxide-years 1859 to 2019: A review of its structure, synthesis, properties and exfoliation," *J. Mater. Chem. C*, vol. 8, no. 5, pp. 1517–1547 (2020).

[5] P. Chamoli, M. K. Das, and K. K. Kar, "Urea-assisted low temperature green synthesis of graphene nanosheets for transparent conducting film," *J. Phys. Chem. Solids*, vol. 113, pp. 17–25 (2018).

[6] J. Phiri, P. Gane, and T. C. Maloney, "General overview of graphene: Production, properties and application in polymer composites," *Mater. Sci. Eng. B Solid-State Mater. Adv. Technol.*, vol. 215, pp. 9–28 (2017).

[7] C. Bulin, Z. Ma, T. Guo, B. Li, Y. Zhang, and B. Zhang, "Journal of Physics and Chemistry of Solids Magnetic graphene oxide nanocomposite: One-pot preparation, adsorption performance and mechanism for aqueous Mn (II) and Zn (II)," vol. 156, no. March (2021).

[8] Z. Dai, Y. Huang, H. Yang, P. Yao, Y. Yang, and C. Ni, "Preparation and biological applications of graphene oxide functionalized water-based magnetic fluids," *J. Nanosci. Nanotechnol.*, vol. 18, no. 1, pp. 735–742 (2018).

[9] S. Pei and H. M. Cheng, "The reduction of graphene oxide," *Carbon N. Y.*, vol. 50, no. 9, pp. 3210–3228 (2012).

[10] S. Hun, "Thermal Reduction of Graphene Oxide," *Phys. Appl. Graphene - Exp.* (2011).

[11] H. Zhou and D. Zhang, "Effects of interactions with metal ions on the thermal reduction of graphene oxide," *J. Phys. Chem. Solids*, vol. 154, no. April 2020, p. 110090 (2021).

[12] K. K. H. De Silva, H. H. Huang, R. K. Joshi, and M. Yoshimura, "Chemical reduction of graphene oxide using green reductants," *Carbon N. Y.*, vol. 119, pp. 190–199 (2017).

[13] E. Aawani, N. Memarian, and H. R. Dizaji, "Synthesis and characterization of reduced graphene oxide–V2O5 nanocomposite for enhanced photocatalytic activity under different types of irradiation," *J. Phys. Chem. Solids*, vol. 125, no. June 2018, pp. 8–15 (2019).

[14] G. K. Ramesha and N. S. Sampath, "Electrochemical reduction of oriented Graphene oxide films: An in situ Raman spectroelectrochemical study," *J. Phys. Chem. C*, vol. 113, no. 19, pp. 7985–7989 (2009).

[15] S. Y. Toh, K. S. Loh, S. K. Kamarudin, and W. R. W. Daud, "Graphene production via electrochemical reduction of graphene oxide: Synthesis and characterisation," *Chem. Eng. J.*, vol. 251, pp. 422–434 (2014).

[16] K. Rahimi and A. Yazdani, "Incremental photocatalytic reduction of graphene oxide on vertical ZnO nanorods for ultraviolet sensing," *Mater. Lett.*, vol. 262, p. 127078 (2020).

[17] S. Taniselass, M. K. Md Arshad, and S. C. B. Gopinath, "Current state of green reduction strategies: Solution-processed reduced graphene oxide for healthcare biodetection," *Mater. Sci. Eng. C*, vol. 96, no. October 2018, pp. 904–914 (2019).

[18] V. Agarwal and P. B. Zetterlund, "Strategies for reduction of graphene oxide – A comprehensive review," *Chem. Eng. J.*,

vol. 405, no. August 2020, p. 127018 (2021).

[19] N. N. Nyangiwe, M. Khenfouch, F. T. Thema, K. Nukwa, L. Kotsedi, and M. Maaza, "Free-Green Synthesis and Dynamics of Reduced Graphene Sheets via Sun Light Irradiation," *Graphene*, vol. 04, no. 03, pp. 54–61 (2015).

[20] Y. Zhang *et al.*, "Facile synthesis of well-dispersed graphene by γ-ray induced reduction of graphene oxide," *J. Mater. Chem.*, vol. 22, no. 26, pp. 13064–13069 (2012).

[21] Y. H. Ding, P. Zhang, Q. Zhuo, H. M. Ren, Z. M. Yang, and Y. Jiang, "A green approach to the synthesis of reduced graphene oxide nanosheets under UV irradiation," *Nanotechnology*, vol. 22, no. 21 (2011).

[22] Marinoiu Adriana *et al.*, "One-step synthesis of graphene supported platinum nanoparticles as electrocatalyst for PEM fuel cells," *Int. J. Hydrogen Energy*, vol. In press, no. In press, p. In press (2020).

[23] G. Williams, B. Seger, and P. V Kamat, "UV-Assisted Photocatalytic Reduction of Graphene Oxide," *ACS Nano*, vol. 2, no. 7, pp. 1487–1491 (2008).

[24] A. Velasco-Hernández, R. A. Esparza-Muñoz, F. J. de Moure-Flores, J. Santos-Cruz, and S. A. Mayén-Hernández, "Synthesis and characterization of graphene oxide - TiO2 thin films by sol-gel for photocatalytic applications," *Mater. Sci. Semicond. Process.*, vol. 114, no. December 2019 (2020).

[25] T. Wu, S. Liu, Y. Luo, W. Lu, L. Wang, and X. Sun, "Nanoscale Surface plasmon resonance-induced visible light photocatalytic reduction of graphene oxide: Using Ag nanoparticles as a plasmonic photocatalyst †," pp. 2142–2144 (2011).

[26] O. Akhavan, "Photocatalytic reduction of graphene oxides hybridized by ZnO nanoparticles in ethanol," *Carbon N. Y.*, vol. 49, no. 1, pp. 11–18 (2010).

[27] S. H. Go, H. Kim, J. Yu, N. H. You, B. C. Ku, and Y. K. Kim, "Synergistic effect of UV and L-ascorbic acid on the reduction of graphene oxide: Reduction kinetics and quantum chemical simulations," *Solid State Sci.*, vol. 84, no. August, pp. 120–125 (2018).

[28] R. Yin, P. Shen, and Z. Lu, "A green approach for the reduction of graphene oxide by the ultraviolet/sulfite process," *J. Colloid Interface Sci.*, vol. 550, pp. 110–116, Aug. (2019).

[29] A. Moosa and J. Noori Jaafar, "Green Reduction of Graphene Oxide Using Tea Leaves Extract with Applications to Lead Ions Removal from Water," *Nanosci. Nanotechnol.*, vol. 7, no. 2, pp. 38–47 (2017).

[30] J. Mangadlao, D. Choi, P.-F. Cao, and R. C. Advincula, "Photoreduction of Graphene Oxide and Photochemical Synthesis of Graphene – Metal Nanoparticle Hybrids by Ketyl Radicals," *Appl. Mater. Interfaces*, vol. 9, no. 29, pp. 24887–24898 (2017).

[31] J. M. D. Tasco, L. Guardia, J. I. Paredes, R. Rozada, and A. Martı, "UV light exposure of aqueous graphene oxide suspensions to promote their direct reduction, formation of graphene – metal nanoparticle hybrids and dye degradation," vol. 0 (2011).

[32] S. Gilje, R. B. Kaner, G. G. Wallace, D. A. N. Li, and M. B. Mu, "Processable aqueous dispersions of graphene nanosheets," pp. 101–105 (2008).

[33] A. De Leon, M. Mellon, J. Mangadlao, and E. Pentzer, "The pH dependent reactions of graphene oxide with small molecule thiols †," pp. 18388–18395 (2018).

[34] W. Ge, Q. Ma, W. Wang, F. Jia, and S. Song, "Synthesis of three-dimensional reduced graphene oxide aerogels as electrode material for supercapacitor application," *Chem. Phys.*, vol. 543, no. October 2020, p. 111096 (2021).

[35] S. Mypati, A. Sellathurai, M. Kontopoulou, A. Docoslis, and D. P. J. Barz, "High concentration graphene nanoplatelet dispersions in water stabilized by graphene oxide," *Carbon N. Y.*, vol. 174, pp. 581–593 (2021).

[36] Y. L. Yu, Y. T. Zhuang, X. Y. Song, and J. H. Wang, "Lyophilized carbon nanotubes/graphene oxide modified cigarette filter for the effective removal of cadmium and chromium from mainstream smoke," *Chem. Eng. J.*, vol. 280, pp. 58–65 (2015).

[37] Y. Tang *et al.*, "Reduced graphene oxide-supported Ni-Mo x C electrocatalyst for hydrogen evolution reaction prepared by ultrasonication and lyophilization," *Int. J. Hydrogen Energy*, vol. 44, no. 18, pp. 9328–9337 (2019).

[38] P. Ribao, M. Alexandra Esteves, V. R. Fernandes, M. J. Rivero, C. M. Rangel, and I. Ortiz, "Challenges arising from the use of TiO2/rGO/Pt photocatalysts to produce hydrogen from crude glycerol compared to synthetic glycerol," *Int. J. Hydrogen Energy*, pp. 1–13 (2018).

[39] S. Liang, Y. Zhou, K. Kang, Y. Zhang, Z. Cai, and J. Pan, "Synthesis and characterization of porous TiO2-NS/Pt/GO aerogel: A novel three-dimensional composite with enhanced visible-light photoactivity in degradation of chlortetracycline," *J. Photochem. Photobiol. A Chem.*, vol. 346, pp. 1–9 (2017).

[40] A. Mannan, Y. Hirano, A. T. Quitain, M. Koinuma, and T. Kida, "Graphene Oxide to B, N Co-doped Graphene through Tris-dimethylaminoborane Complex by Hydrothermal Implantation," *Am. J. Mater. Sci.*, vol. 9, no. 1, pp. 22–28 (2019).

[41] I. Childres, L. A. Jauregui, W. Park, H. Caoa, and Y. P. Chena, "Raman spectroscopy of graphene and related materials," *New Dev. Phot. Mater. Res.*, pp. 403–418 (2013).

[42] C. Klinke, R. Kurt, J. M. Bonard, and K. Kern, "Raman spectroscopy and field emission measurements on catalytically grown carbon nanotubes," *J. Phys. Chem. B*, vol. 106, no. 43, pp. 11191–11195 (2002).

[43] K. Haubner *et al.*, "The route to functional graphene oxide," *ChemPhysChem*, vol. 11, no. 10, pp. 2131–2139 (2010).

[44] J. M. Sunil Meti, Udaya Bhat K., Rahman M. R., "Photocatalytic Behaviour of Nanocomposites of Sputtered Titanium Oxide Film on Graphene Oxide Nanosheets," *Am. J. Mater. Sci.*, vol. 5, no. October, pp. 12–18 (2015).

[45] R. Ramachandran, S. Felix, G. M. Joshi, B. P. C. Raghupathy, S. K. Jeong, and A. N. Grace, "Synthesis of graphene platelets by chemical and electrochemical route," *Mater. Res. Bull.*, vol. 48, no. 10, pp. 3834–3842 (2013).

[46] S. S. Rajabzoda *et al.*, "Efficient solvothermal reduction of coarse-scale graphene oxide," *J. Phys. Chem. Solids*, vol. 140, no. July 2019, p. 109259 (2020).

[47] A. Bayrakçeken Yurtcan and E. Daş, "Chemically synthesized reduced graphene oxide-carbon black based

hybrid catalysts for PEM fuel cells," *Int. J. Hydrogen Energy*, vol. 43, no. 40, pp. 18691–18701, Oct. (2018).

[48] M. Tavafoghi, N. Brodusch, R. Gauvin, and M. Cerruti, "Hydroxyapatite formation on graphene oxide modified with amino acids: Arginine versus glutamic acid," *J. R. Soc. Interface*, vol. 13, no. 114 (2016).